Fluctuation Corrections for Correlated Random Copolymers

Henk Angerman and Gerrit ten Brinke*

Department of Polymer Chemistry and Materials Science Centre, University of Groningen Nijenborgh 4, 9747 AG Groningen, The Netherlands

Igor Erukhimovich*

Department of Physics, Moscow State University, Moscow 117234, Russia

Received January 27, 1997; Revised Manuscript Received January 22, 1998

ABSTRACT: Fluctuation effects on the order−disorder transition (ODT) in correlated random copolymers (polydisperse A/B multiblock copolymers with block lengths having an exponential Flory distribution, and a large average number of blocks per chain) are studied with due regard for the strong temperature dependence of the period of the arising ordered phases, characteristic for the system under consideration. To this end, following a field theoretical variational method, the free energy is minimized with respect to both the concentration profile ψ and the correlation function G, assumed to belong to certain classes of trial functions. The trial function for G contains an extra adjustable parameter as compared to the situation typical for monodisperse A/B block copolymer melts. The shape of the correlation function and its temperature dependence are determined both for the disordered phase and for the ordered phases. In the vicinity of the critical point the phase diagram is calculated and presented in a universal form by using reduced variables. It is shown that near the ODT and for A-monomer fractions f close to $^1/_2$, the profiles are strongly fluctuating: in the ordered phase the amplitude of the fluctuations is equal to the amplitude of the average profile, and in the disordered phase the concentration inhomogeneities are comparable to those in the ordered phase. In the same region the disordered phase has an anomalously large correlation length, indicating some kind of local ordering. In connection with this, we discuss the close relationship between the disordered phase and the random wave structure.

1. Introduction

It is well-known that the homogeneous state of multicomponent polymer mixtures and melts is rarely stable with respect to the occurrence of considerable concentration inhomogeneities. Even the presence of a rather small segregating short-range interaction (usually described by the Flory−Huggins χ-parameter[1]) between the different monomers may result in a considerable spatial rearrangement of the macromolecules due to the smallness of their translational entropy. For instance, blends of homopolymers will often undergo separation into two or more coexisting phases.[1,2] Although the compositions of these phases differ from the overall composition, each phase separately is homogeneous. However, before achieving this locally homogeneous state, the system exhibits long-lived large-scale transient inhomogeneities (Cahn−Hilliard waves).

In contrast, melts of monodisperse block copolymers undergo an order−disorder transition[3−5] (ODT), which requires a rearrangement of the polymer molecules on length scales of the size of their blocks only and is, therefore, a much faster process, which results in thermodynamically stable inhomogeneities having the symmetry of a crystal group.

Random copolymers form a very interesting intermediate class of copolymers revealing a rather peculiar way of destroying the homogeneous state. As shown first by Shakhnovich and Gutin,[6] mean-field theory predicts a transition to a microphase-separated state. The period L of the microstructure was found to be strongly dependent on the temperature T via $L \propto 1/\sqrt{T_s - T}$, where T_s is the spinodal temperature. The period is anomalously large and approaches infinity at the spinodal, which justifies considering the order−disorder transition in random copolymers within the framework of the weak segregation approach. The temperature dependence of L coincides with that of the length of the Cahn−Hilliard waves appearing during the spinodal decomposition of the corresponding system of disconnected monomers (i.e., the same system, but without the presence of the chemical bonds). Therefore, it was suggested in refs 5 and 12 that the spatial structure in a random copolymer melt below the mean-field transition temperature may be considered as having the pattern of the spinodal decomposition in the corresponding system of disconnected monomers, stabilized due to the presence of the chemical bonds randomly distributed among these monomers. This physical picture clarifies the fluctuating disordered nature of the concentration profile in random copolymer melts (see below).

In this paper we study the phase behavior of a *correlated* random copolymer melt; see refs 11, 19, 20, 22, and 26. In a correlated random copolymer, the probability of finding a monomer of type α = A/B depends on the neighboring monomers along the chain. We assume a positive chemical correlation, leading to long sequences of identical monomers. For large values of the characteristic length l of these sequences, the mean-field phase diagram has been calculated before[19,20] and is presented in Figure 1. The period L of the microstructure arising in a correlated random copolymer melt has the same strong temperature dependence[26] as that for the uncorrelated random copolymer. When

S0024-9297(97)00105-8 CCC: $15.00
Published on Web 03/05/1998

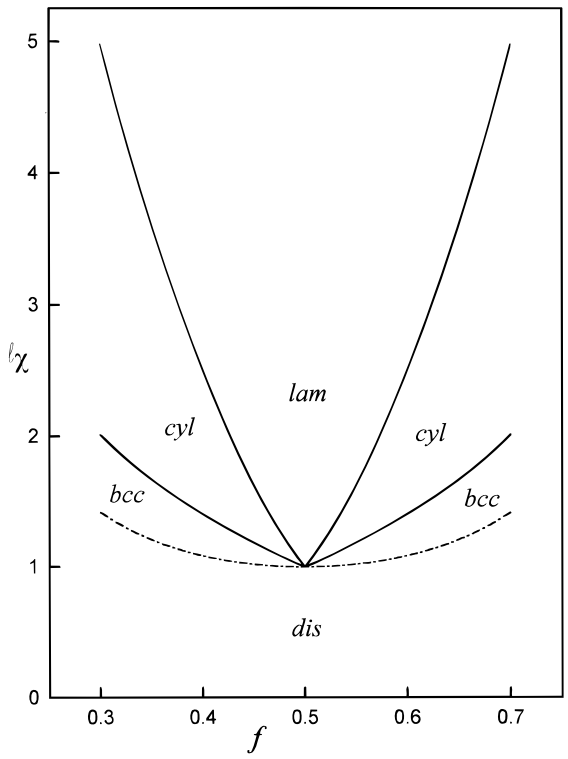

Figure 1. Mean-field phase diagram for the correlated random copolymer. Horizontal: A-monomer fraction f. Vertical: rescaled interaction strength $l\chi$. Dashed line: third-order transition. Solid line: first-order transition.

compared with the phase diagrams of monodisperse regular block copolymers,[7,21] the phase diagram of random copolymers has a much larger region of stability of the bcc phase, and a bend in the phase boundaries at the point $f_A = f_B = {}^1/_2$. (f_α is the fraction of monomers of type α.) As first shown in ref 22, the order−disorder transition is third order over the entire interval $0.17 < f_A < 0.83$, and first order outside this interval.

This mean-field picture needs adjustment when fluctuation corrections are taken into account, which was done for the first time in ref 10 for the case of uncorrelated random copolymers. Generally, for block copolymer melts fluctuations become less important as the average block length N increases ($N \approx l$ for a correlated random copolymer). Consequently, for an *un*correlated random copolymer ($l \approx 1$), the fluctuation corrections are considerable. One of the consequences is an increase in the region of stability of the disordered phase, which can be measured by the shift $\Delta\chi > 0$ of the phase transition line. For monodisperse[23] regular block copolymers $\Delta(N\chi) \propto N^{-1/3}$, whereas for correlated[18] random copolymers $\Delta(N\chi) \propto N^{-1/4}$. This relatively slow decrease of the fluctuation corrections is due to a peculiar property of the free energy of the random copolymer: both for correlated and for uncorrelated random copolymers the dominant contribution H_0 to the Landau Hamiltonian H is degenerate with respect to the morphology of the microstructure; in other words, all morphologies have exactly the same value for H_0. If the subdominant contributions to H are neglected, the fluctuation corrections destroy completely the stability of the ordered phases, and the disordered phase becomes thermodynamically stable everywhere, which was proven mathematically in refs 12, 13, and 16 and via Monte Carlo simulations in ref 14. For $T < T_s$ (where T_s is the spinodal temperature) this disordered phase has an anomalously large correlation length.[12] Moreover, although $\langle\psi\rangle = 0$, the system is far from homogeneous due to the strong fluctuations. In this respect, the disordered phase for $T < T_s$ resembles a disordered microstructure[11] ("random wave structure").

As was shown by Erukhimovich and Dobrynin[16,17] by studying a phenomenological Hamiltonian, the presence of a small degeneracy-breaking term makes a transition to an ordered phase possible. Nevertheless, it was also shown that a *near*-degeneracy has implications for the phase behavior: due to fluctuations, the region of stability of the disordered phase increases if the degeneracy-breaking term becomes smaller. For random copolymers, the relative magnitude of this term decreases to zero on approaching the spinodal, making the system completely degenerate at the spinodal itself. This effect accounts for the slow decrease of the fluctuations in the correlated random copolymer as expressed by $\Delta(N\chi) \propto N^{-1/4}$.

This discussion motivates the objective of our paper: to improve our understanding of the order−disorder transition in correlated random copolymer melts via a quantitative treatment of the fluctuation corrections. To this end, the paper is organized as follows. In section 2 a precise definition of the model will be given. In section 3 we present a modification of the general procedure to calculate fluctuation corrections via a variational approach.[24] In section 4 we study the phase behavior in the limit $l \to \infty$. In section 5 we present the fluctuation corrections to the phase diagram in the vicinity of the critical point for large (but finite) values of l and calculate the amplitude of the fluctuations in the profiles. The implications of the results obtained and the conditions of their validity are discussed in the Conluding Remarks.

2. Model

We consider an incompressible highly polydisperse multiblock copolymer melt consisting of two sorts of monomers, denoted by A and B. The statistical segment lengths a of the A−A, A−B, and B−B bonds are assumed to be the same, and $a/\sqrt{6}$ is chosen as the unit of length. Also the excluded volumes v of the A- and B-monomers are the same and given by

$$v^{1/3} = \frac{a}{\sqrt{6}} = 1 \tag{2.1}$$

The average number of blocks per macromolecule is assumed to be so large that its inverse value may be neglected. Following ref 11, we describe the monomer sequence distribution of this multiblock copolymer by a first-order Markov process characterized by conditional probabilities $p_{\alpha\beta}$, which are defined as the probability of finding a monomer of type α, given that its left neighbor is of type β. Since every monomer must be either of type α or of type β, the conditional probabilities $p_{\alpha\beta}$ satisfy the constraints

$$p_{AA} + p_{BA} = 1$$
$$p_{AB} + p_{BB} = 1 \tag{2.2}$$

Equation 2.2 leaves only two independent probabilities: p_{AA} and p_{BB}, which determine an exponential Flory

distribution of the A- and B-blocks. If $w_\alpha(n)$ denotes the probability that a randomly picked block of type α = A/B consists of n monomers, then

$$w_\alpha(n) = (1 - p_{\alpha\alpha})p_{\alpha\alpha}^{n-1} \approx \frac{e^{-n/n_\alpha}}{n_\alpha}$$

$$n_\alpha = \frac{\sum_n n w_\alpha(n)}{\sum_n w_\alpha(n)} = (1 - p_{\alpha\alpha})^{-1} \qquad (2.3)$$

where n_α is the average number of monomers per block of type α. It is useful to express the two independent probabilities p_{AA} and p_{BB} in terms of the average monomer fraction f and the parameter λ characterizing the chemical correlation between neighboring monomers. To this end, we consider two neighboring monomers and express the probability that the right one is of type α (which equals, evidently, the average fraction f_α of the monomers of this type) in terms of the two possibilities for the chemical identity of the left one:

$$f_A = f_B p_{AB} + f_A p_{AA}$$

$$f_B = f_A p_{BA} + f_B p_{BB} \qquad (2.4)$$

Note that in deriving eq 2.4 it is assumed that there are no (or negligibly few) monomers having less than two neighbors. Putting it in other words, the copolymer chains are assumed to be infinitely long. When written in matrix notation, eq 2.4 shows that 1 is an eigenvalue of the matrix $p_{\alpha\beta}$ and ($f_A = f$, $f_B = 1 - f$) is the corresponding eigenvector. The other eigenvalue of the matrix is

$$\lambda = p_{AA} + p_{BB} - 1 \qquad (2.5)$$

The parameters f and λ describe the Markov process completely. We assume in this paper that the molecules contain long sequences of like monomers:

$$1 - p_{AA} = n_A^{-1} \ll 1 \qquad 1 - p_{BB} = n_B^{-1} \ll 1$$

$$1 - \lambda = 2 - p_{AA} - p_{BB} = n_A^{-1} + n_B^{-1} \ll 1 \qquad (2.6)$$

Since λ is close to unity, it is more convenient to describe the sequence distribution in terms of the chemical correlation length l. It is defined by[22]

$$l \equiv (1 - \lambda)^{-1} = (2 - p_{AA} - p_{BB})^{-1} = (n_A^{-1} + n_B^{-1})^{-1} \qquad (2.7)$$

The length l is closely related to the average block lengths n_α, and further on we will refer to l simply as the "block scale". With eqs 2.2 and 2.4 the parameter f can be expressed in terms of p_{AA} and p_{BB}:

$$f = \frac{1 - p_{BB}}{2 - p_{AA} - p_{BB}} \qquad (2.8)$$

All properties of the correlated random copolymer (CRC) model under consideration can be expressed in terms of f, l, and the Flory–Huggins parameter χ describing the interaction between the A- and B-monomers. Realizing that the degree of segregation in multiblock copolymers is determined by the interaction per block rather than the interaction per monomer, it is more convenient to characterize it via the parameter

$$t \equiv l\,(\chi - \chi_s) \qquad (2.9)$$

where χ_s is the spinodal value of χ. For nearly symmetric correlated random copolymers it can be approximated by

$$l\chi_s \cong l\chi_c = 1 \qquad (2.10)$$

where χ_c is the critical value for χ.

3. Theory

In order to calculate the phase diagram, it has to be determined which state (either disordered or having a spatial symmetry) is thermodynamically stable for a given value of f and $l\chi$. An ordered state is characterized by a nonzero expectation value $\langle\psi\rangle$ of the concentration profile ψ defined by

$$\psi(\vec{x}) = \rho_A(\vec{x}) - \langle\rho_A\rangle \qquad (3.1)$$

where $\rho_A(\vec{x})$ is the local density of A-monomers. To find the phase diagram, the free energy is required:

$$F(f, \chi) = -k_B T \ln Z(f, \chi) \qquad (3.2)$$

where T is the temperature, k_B is Boltzmann's constant, and Z is the partition function defined as the integral over all possible profiles $\psi(\vec{x})$

$$Z = \int \delta\psi \exp[-H[\psi(\vec{x})]/k_B T] \qquad (3.3)$$

where the effective Hamiltonian $H[\psi(\vec{x})]$ is the "virtual" free energy of the state with given profile $\psi(\vec{x})$. Both entropic and energetic contributions are included in H. From here on we restrict ourselves to the weak segregation regime where, by definition, $\psi(\vec{x})$ is small, which means that the density $\rho_A(\vec{x})$ differs only slightly from its average value. In this case, the virtual free energy may be approximated by its Landau expansion in powers of ψ. Because of the translational invariance, this expansion starts at second order:

$$H[\psi] \approx F_L[\psi] = k_B T \sum_{n=2}^{n=4} \frac{1}{n!} \int d\vec{x}_1 \ldots d\vec{x}_n \times \Gamma_n(\vec{x}_1, \ldots, \vec{x}_n)\, \psi(\vec{x}_1) \ldots \psi(\vec{x}_n)$$

$$= k_B T \sum_{n=2}^{n=4} \frac{1}{n! V^n} \sum_{\vec{q}_1 \ldots \vec{q}_n} \tilde{\Gamma}_n(\vec{q}_1, \ldots, \vec{q}_n) \times \tilde{\psi}(-\vec{q}_1) \ldots \tilde{\psi}(-\vec{q}_n) \qquad (3.4)$$

The tildes on the Fourier transforms will be omitted, because the distinction between a function and its Fourier transform will be clear from its argument. The vertex functions Γ_n can be expressed in terms of the correlation functions G_n, which should be averaged over all molecule types present in the polydisperse CRC. These correlation functions allow for spatial and chemical correlations among the monomers A and B pertaining to the chains forming the CRC. These chains are assumed to obey Gaussian statistics. This assumption—the famous Flory theorem—is widely accepted and verified (by theoretical and experimental

means and by computer simulations) for concentrated polymer systems far away from the ODT in the disordered state. It may be shown that the non-Gaussian perturbations of the chains are automatically included when the fluctuation corrections are calculated via the variational approach. The vertices Γ_n for the CRC have been presented in refs 19, 20, and 22. For the second- and third-order vertices, the result is

$$\Gamma_2(\vec{q}_1, \vec{q}_2) = V\delta_K(\vec{q}_1 + \vec{q}_2)\,\gamma_2(q_1)$$
$$\Gamma_3(\vec{q}_1, \vec{q}_2, \vec{q}_3) = V\delta_K(\vec{q}_1 + \vec{q}_2 + \vec{q}_3)\,\gamma_3(\vec{q}_1, \vec{q}_2, \vec{q}_3)$$

$$\gamma_2(q) = \frac{1 + lq^2}{2lf(1-f)} - 2\chi$$
$$\gamma_3(\vec{q}_1, \vec{q}_2, \vec{q}_3) = \frac{(f - 1/2)(3 + l{q_1}^2 + l{q_2}^2 + l{q_3}^2)}{2lf^2(1-f)^2} \quad (3.5)$$

The expression for the fourth-order vertex is more complicated. Quite generally, for polydisperse systems it can be written as a sum of two contributions.[6,25−27] The first (regular) contribution γ_4^{reg} is just the generalization of the expression of the fourth-order vertex for monodisperse copolymers. The second contribution γ_4^{nl} is the nonlocal term, which is only present for polydisperse systems. Generally, one can write

$$\Gamma_4(\vec{q}_1, \vec{q}_2, \vec{q}_3, \vec{q}_4) = V\delta_K(\vec{q}_1 + \vec{q}_2 + \vec{q}_3 + \vec{q}_4) \times$$
$$[\gamma_4^{reg}(\vec{q}_1 + \vec{q}_2 + \vec{q}_3 + \vec{q}_4) + \delta_K(\vec{q}_1 + \vec{q}_2)\,\gamma_4^{nl}(q_1, q_3) +$$
$$\delta_K(\vec{q}_1 + \vec{q}_3)\,\gamma_4^{nl}(q_1, q_2) + \delta_K(\vec{q}_1 + \vec{q}_4)\,\gamma_4^{nl}(q_1, q_2)] \quad (3.6)$$

For the correlated random copolymer, the expressions for γ_4^{reg} and γ_4^{nl} are given by

$$\gamma_4^{reg}(\vec{q}_1, \vec{q}_2, \vec{q}_3, \vec{q}_4) =$$
$$\frac{3(5-16f+16f^2)+4(1-3f+3f^2)(l{q_1}^2+l{q_2}^2+l{q_3}^2+l{q_4}^2)}{8lf^3(1-f)^3}$$

$$\gamma_4^{nl}(q_1, q_2) = \frac{8f(1-f) + lq^2(3 + lq^2)}{8lf^3(1-f)^3\, lq^2(1 + lq^2)} \qquad q^2 \equiv {q_1}^2 + {q_2}^2 \quad (3.7)$$

Remarkably, the expressions for the third-order vertex and for the regular part of the fourth-order vertex do not depend on the angles between the vectors. To construct the phase diagram in the vicinity of the critical point, it is necessary to know the vertex functions near $f = 1/2$ only. After the vertex functions are expanded in powers of $\epsilon \equiv f - 1/2$, the question arises which terms in this expansion should be included and which can be neglected. The answer can be found in the mean-field phase diagram shown in Figure 1. The transitions between the various ordered phases take place for A-monomer fractions that satisfy the scaling $|\epsilon| \propto t \equiv l(\chi - \chi_s)$. Moreover, in the neighborhood of the critical point, the amplitude A and the inverse period q_* of the structure satisfy the scaling $A \propto l{q_*}^2 \propto t$. It is now clear that in the weak segregation regime one has to take into account all terms in the expansion of the free energy up till the fourth order in the parameters A, $l{q_*}^2$, t, and ϵ. With this rule, the final expressions are given by

$$\gamma_2(\vec{q}) = 2q^2 - \frac{2t}{l} \qquad \gamma_3(\vec{q}_1, \vec{q}_2, \vec{q}_3) = \frac{24\epsilon}{l}$$

$$\gamma_4^{reg}(\vec{q}_1, \vec{q}_2, \vec{q}_3, \vec{q}_4) = \frac{24}{l} \qquad \gamma_4^{nl}(q^2) = \frac{16}{l^2q^2} + \frac{8}{l}$$

$$\epsilon = f - \frac{1}{2} \qquad t = l(\chi - \chi_c) \quad (3.8)$$

This is a good place to stress two important features of the Landau Hamiltonian for correlated random copolymer melts:

The minimum of the second vertex $\gamma_2(q)$ is located at $q = 0$, as first shown in refs 6 and 9 for continuous and discrete copolymer models, respectively.

The fourth vertex contains the "nonlocal term" γ_4^{nl} presented first in ref 6 and in the most general form in refs 25 and 26 (see also refs 11 and 27). Due to its $1/q^2$ dependence, the nonlocal term suppresses the long wavelength concentration fluctuations in the random copolymer. Therefore, the tendency to macrophase separate, which results from the location of the minimum of the second-order vertex[7−9] is suppressed and transformed into the tendency to microphase separate. This will be discussed in more detail in sections 4 and 5.

If $\bar{\psi}(\vec{x})$ is defined to be the profile that minimizes F_L, then the partition function Z is determined by the integration in the vicinity of $\bar{\psi}(\vec{x})$. In the mean-field approximation, the contribution to Z of all profiles $\psi(\vec{x}) \neq \bar{\psi}(\vec{x})$ is neglected and the free energy is given by

$$F_{mean-field} = \min_{\{\psi(x)\}} F_L[\psi] = F_L[\bar{\psi}] \quad (3.9)$$

As discussed already in the Introduction, for the correlated random copolymer the mean-field approximation becomes more accurate if the block scale l increases. For small values of l, the profiles ψ close to $\bar{\psi}$ will also give a considerable contribution to the integral given in eq 3.3, and so eq 3.9 for the free energy needs to be modified. As shown first by Brazovskii[28] (see also refs 23 and 29), the corresponding fluctuation corrections for the weak segregation limit of the ODT can be treated within the Hartree approximation. An efficient tool to implement the corresponding calculations is the field-theoretical variational procedure based on the second Legendre transformation,[30] developed and applied to the ODT in ref 24. According to this procedure, the exact value of the free energy with due regard for the fluctuation corrections may be represented as follows:

$$F = \min_{\{\psi(\vec{x})\},\{G(\vec{x},\vec{y})\}} \tilde{F}[\{\psi(\vec{x})\}, \{G(\vec{x}, \vec{y})\}] \quad (3.10)$$

If the functional $\tilde{F}$ attains its minimum for $\{\psi = \psi_0, G = G_0\}$, then ψ_0 is the average profile and G_0 is the renormalized correlation function:

$$\psi_0(\vec{x}) = \langle\psi(\vec{x})\rangle$$

$$G_0(\vec{x}, \vec{y}) = \langle\psi(\vec{x})\,\psi(\vec{y})\rangle - \langle\psi(\vec{x})\rangle\,\langle\psi(\vec{y})\rangle \quad (3.11)$$

where the brackets $\langle\cdots\rangle$ denote a thermodynamic average. The functional $\tilde{F}[\psi, G]$ is defined as follows:

$$\tilde{F}[\psi, G] = F_L[\psi] + D[G] + \sigma[\psi, G] \quad (3.12)$$

The fluctuation corrections to the free energy in the

"one-loop" approximation are described by the functional

$$D = \frac{1}{2V}\int \mathrm{d}\vec{x}_1\,\mathrm{d}\vec{x}_2\,\Gamma_2(\vec{x}_1,\vec{x}_2)\,G(\vec{x}_1,\vec{x}_2) - \frac{1}{2V}\,\mathrm{Tr}\,\ln G(\vec{x}_1,\vec{x}_2) \quad (3.13)$$

All remaining fluctuation corrections are given by the functional $\sigma[\psi, G]$, which is an infinite series of integrals of powers of ψ and G (the terms in this series may be described and calculated in accordance with certain strict rules ("diagram technique") presented, for instance, in ref 24). In particular, within the framework of the conventional Brazovskii−Fredrickson−Helfand approximation, only two terms of the infinite series are relevant,[24] namely

$$\sigma[\psi, G] \cong D_1 + D_2 \quad (3.14)$$

$$D_1 = \frac{1}{8V}\int \mathrm{d}\vec{x}_1\,\mathrm{d}\vec{x}_2\,\mathrm{d}\vec{x}_3\,\mathrm{d}\vec{x}_4\,\Gamma_4(\vec{x}_1,\vec{x}_2,\vec{x}_3,\vec{x}_4)\times G(\vec{x}_1,\vec{x}_2)\,G(\vec{x}_3,\vec{x}_4) \quad (3.14a)$$

$$D_2 = \frac{1}{4V}\int \mathrm{d}\vec{x}_1\,\mathrm{d}\vec{x}_2\,\mathrm{d}\vec{x}_3\,\mathrm{d}\vec{x}_4\,\Gamma_4(\vec{x}_1,\vec{x}_2,\vec{x}_3,\vec{x}_4)\times G(\vec{x}_1,\vec{x}_2)\,\psi(\vec{x}_3)\,\psi(\vec{x}_4) \quad (3.14b)$$

To carry out the minimization procedure of $\tilde{F}[\psi, G]$, one should substitute for ψ and G certain plausible trial functions containing suitable adjustable parameters, calculate the integrals appearing in eqs 3.13 and 3.14, and minimize the obtained expression with respect to the adjustable parameters. For ψ we take the first harmonic approximation

$$\langle\psi(\vec{x})\rangle = \frac{A}{\sqrt{k}}\sum_{\vec{Q}} \mathrm{e}^{i\vec{Q}\cdot\vec{x}+\varphi_Q} \quad (3.15)$$

For a given lattice symmetry, the summation runs over the set $\{\vec{Q}\}$ of vectors belonging to the first coordination sphere of the reciprocal lattice. The integer k is half the number of such vectors, and φ_Q is the corresponding phase. The trial function eq 3.15 contains as adjustable parameters the chosen lattice symmetry of the set of vectors $\{\vec{Q}\}$, their phases φ_Q, and their common amplitude A and length Q_*.

The situation with respect to the choice of the class of trial functions for G is not so straightforward. The usual choice is

$$G^{-1}(\vec{q}) = c(q - q_*)^2 + r \quad (3.16)$$

When using the variational procedure presented, this choice proved to be suitable for the case of monodisperse block copolymers where the parameter q_* is mainly determined by the architecture of the system and only slightly depends on the degree of segregation.[7−9] In this case the integrals, eqs 3.13 and 3.14 may be well-defined despite the fact that they are divergent in the large-q region.[24] This is not the case for the correlated random copolymer where all parameters c, r, and q_* are expected to have a strong temperature dependence. So, in this paper we use a different class of trial functions for G, namely

$$G^{-1}(q) = 2q_*^2\left(p^2 + \frac{s^2}{p^2 - 1 + s} - 1 - s + \rho\right) \equiv 2q_*^2\,\widehat{G}^{-1}(p) \qquad p \equiv \frac{q}{q_*} \quad (3.17)$$

which contains three adjustable parameters ρ, s, and q_*. The influence of the parameters s and ρ on the shape of the correlation function $\widehat{G}(p)$ is shown in Figure 2. Note that for $s > 1$ there is some residual forward scattering, which is due to the polydispersity.[36] The important simplifying assumption for both sets of trial functions eqs 3.16 and 3.17 is their isotropic form, which may not be completely correct for the ordered phases. The advantage of the trial function eq 3.17 is the possibility of evaluating the position, height, and width of the peak of the correlation function as independent parameters, which gives a better estimate for the free energy. Moreover, its rational form makes it possible to calculate the integrals in eqs 3.13 and 3.14 analytically. A final remark concerning the adjustable parameters is that, in general, the values of the parameters Q_* and q_* appearing in the trial functions for ψ and G, respectively, may be slightly different. However, in the weak segregation limit they will not differ much and we assume that $Q_* = q_*$. Therefore, both the position of the maximum scattering in the system, and the periodicity of the microstructure are determined by one and the same parameter q_*.

Further on, the expression for $G(\vec{x})$ is required as well. Straightforward calculation shows that it is an exponentially decaying sine given by

$$G(\vec{x}) = \frac{s\mathrm{e}^{-bq_*x}}{16\pi a\,b\,x}\sin[aq_*x + \varphi] \qquad \varphi = \arccos\left[1 - \frac{\rho}{2s}\right]$$

$$a = \frac{\sqrt{1 - \rho/2 + \sqrt{1 - \rho + \rho s}}}{\sqrt{2}}$$

$$b = \frac{\sqrt{-1 + \rho/2 + \sqrt{1 - \rho + \rho s}}}{\sqrt{2}} \quad (3.18)$$

$G(\vec{x})$ is characterized by two length scales: $R_{\mathrm{osc}} = 1/aq_*$, which is proportional to the period of the oscillations, and $R_{\mathrm{cor}} = 1/bq_*$, which is the correlation length.

4. Phase Behavior in the Limit of Infinite Average Block Length

In this section we study the ordered phases and the disordered phase in the region of the phase diagram, which is defined by the following two criteria: (1) the system is weakly segregated; (2) the fluctuations in the ordered phases are negligible. The first condition implies that the distance to the critical point is not too large, and the second implies that it is not too small. The first is satisfied by taking small values for ϵ and t, whereas the second can only be satisfied at the same time if the fluctuation region is small, which will be the case if l is large. Therefore, in this section we consider the limit $l \to \infty$, in which case the second criterion is satisfied for all $\epsilon > 0$, $t > 0$.

The purpose of this paragraph is to find the shape of the correlation function $G(q)$ and to describe the supercooled disordered phase. Although for the ordered phases the mean-field theory is exact in the limit $l \to \infty$, in order to obtain information about the correlation

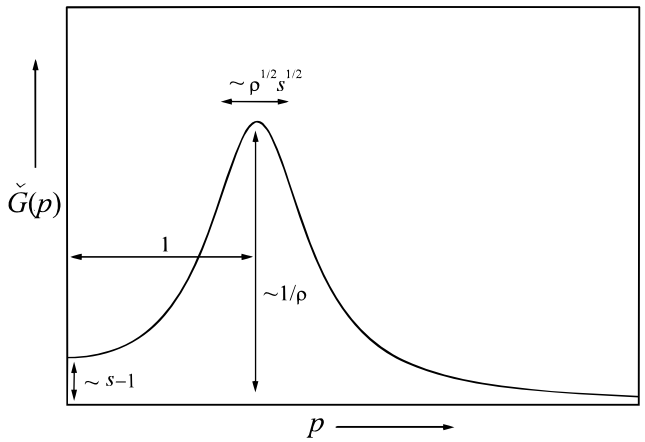

Figure 2. Influence of the parameters ρ and s on the shape of the correlation function. Horizontal: rescaled q-value $p \equiv q/q_*$.

function it is nevertheless necessary to take the (negligible) fluctuation corrections into account, because the mean-field free energy does not depend on $G(q)$.

Ordered Phases. To be able to determine which terms in the free energy expansion have to be included and which can be neglected, we assume that the adjustable parameters A, q_*, ρ and s satisfy the scaling laws

$$A \propto l^0, \quad q_* \propto l^{-1/2}, \quad \rho \propto l^0, \quad s \propto l^0 \tag{4.1}$$

The scaling behavior for A and q_* was already derived in refs 19, 20, and 22, whereas the scaling relations for ρ and s will be verified by the fact that the subsequent calculations result in explicit expressions for the parameters ρ and s, which indeed satisfy eq 4.1. In the free energy expansion in powers of l^{-1}, we keep only the leading mean-field contribution F_0 (which is independent of ρ and s) and the next term F_1:

$$F = F_0(A, q_*) + F_1(A, q_*, \rho, s) + O(l^{-2})$$

$$F_0 \propto l^{-1} \qquad F_1 \propto l^{-3/2} \tag{4.2}$$

With the vertex functions given in eq 3.8, the mean-field contribution F_0 can be written down:

$$lF_0 = 2(lq^2 - t)A^2 + \frac{4A^4}{lq^2} - 24\mu|\epsilon|A^3 + \lambda A^4 \tag{4.3}$$

The parameters μ and λ depend on the morphology of the microstructure. For the lamellar, cylindrical, bcc phase, and the random wave structure[11] they are given by

$$\mu_{\text{lam}} = 0 \qquad \mu_{\text{hex}} = 2/3\sqrt{3} \qquad \mu_{\text{bcc}} = 4/3\sqrt{6} \qquad \mu_{\text{ran}} = 0$$

$$\lambda_{\text{lam}} = 10 \qquad \lambda_{\text{hex}} = 14 \qquad \lambda_{\text{bcc}} = 19 \qquad \lambda_{\text{ran}} = 16 \tag{4.4}$$

The random wave structure (also called the *disordered microstructure*) proposed in ref 11 is defined as the structure having the following form of the concentration profile $\langle\psi\rangle$:

$$\langle\psi(\vec{x})\rangle = \frac{A}{\sqrt{k}} \sum_{\vec{Q}} \exp(\vec{Q}\cdot\vec{x} + \varphi_Q) \tag{4.5}$$

with the vectors $\vec{Q}$ randomly distributed over the unit sphere. The phases φ_Q are also random. The number $2k$ of vectors $\vec{Q}$ in the first coordination sphere approaches infinity. Since the vectors $\vec{Q}$ have random directions, there are no triples adding up to zero, and therefore, the third-order coefficient μ is zero. To find the fourth-order coefficient λ, one has to identify the quadruples $(\vec{Q}_1, \vec{Q}_2, \vec{Q}_3, \vec{Q}_4)$ satisfying $\sum\vec{Q}_i = 0$, where $\vec{Q}_i$ belongs to the first coordination sphere. Since the vectors $\vec{Q}$ have random directions, the only quadruples satisfying this condition are of the form $(\vec{Q}_1, -\vec{Q}_1, \vec{Q}_2, -\vec{Q}_2)$, or $(\vec{Q}, \vec{Q}, -\vec{Q}, -\vec{Q})$. The number of ordered quadruples of the first type is equal to $4!k(k-1)/2$, whereas the number of quadruples of the second type is equal to $6k$. Due to the fact that the regular part γ_4^{reg} of the fourth-order vertex does not depend on the angles between the vectors (see eq 3.7 and refs 19 and 20), the corresponding value of λ can be written down easily:

$$\lim_{k\to\infty} \frac{1}{4!k^2V}\left(\frac{4!k(k-1)}{2}\Gamma_4(\vec{Q}_1, -\vec{Q}_1, \vec{Q}_2, -\vec{Q}_2) + 6k\Gamma_4(\vec{Q}, \vec{Q}, -\vec{Q}, -\vec{Q})\right) = \frac{1}{2V}\Gamma_4(\vec{Q}_1, -\vec{Q}_1, \vec{Q}_2, -\vec{Q}_2) = \frac{4}{l^2{q_*}^2} + \frac{16}{l} \Rightarrow \lambda_{\text{ran}} = 16 \tag{4.6}$$

When the free energy eq 4.3 is minimized with respect to the parameters A and q_*, the result is (up to the adopted accuracy)

$$A_0 = \frac{t}{3\sqrt{2}} + \mu|\epsilon|t - \frac{\lambda t^2}{54\sqrt{2}} \qquad l{q_0}^2 = A_0\sqrt{2}$$

$$lF_0 = -\frac{t^3}{27} + \frac{\lambda t^4}{324} - \frac{2\sqrt{2}\,\mu|\epsilon|t^3}{9} \tag{4.7}$$

Because of the inequality $\lambda_{\text{lam}} < \lambda_{\text{ran}}$, the free energy of the random wave structure is never below that of the lamellar structure, and therefore, the random wave structure can exist only as a metastable state. Equation 4.7 for the free energy of the ordered phases shows that in the (ϵ, t)-plane near the critical point the phase transition lines separating the regions of stability of the different phases are straight lines. The slope of these lines can be found by solving the equations $F_0(\text{lam}) = F_0(\text{cyl})$ and $F_0(\text{bcc}) = F_0(\text{cyl})$. It follows[19,20]

$$\frac{t_{nm}}{|\epsilon|} = \frac{l(\chi_{nm} - \chi_c)}{\left|f - \frac{1}{2}\right|} = 72\sqrt{2}\,\frac{\mu_n - \mu_m}{\lambda_n - \lambda_m} \approx \begin{cases} 3.247 & \text{for the bcc/cyl border} \\ 9.798 & \text{for the cyl/lam border} \end{cases} \tag{4.8}$$

The corresponding mean-field phase diagram is shown in Figure 1. As presented in ref 22, the analysis of the free energy further away from the critical point shows that the transition from the disordered phase to the bcc phase is a third-order transition not only in the critical point but in the interval $f_c < f < 1 - f_c$, with $f_c = 0.173$. Thus, it is only a matter of convention that we refer to $(\epsilon = 0, t = 0)$ as the critical point.

The leading order fluctuation correction F_1 is the sum of the contributions D and D_2 defined by eqs 3.13 and 3.14b; it is calculated in Appendix A. The term D_1 can

be neglected in this section because it is proportional to l^{-2}, which follows from (A3) and (A4), using eq 4.1. The expressions for D and D_2 are given in terms of the integrals I_4, I_6, and I_9 evaluated in Appendix B:

$$F_1 = \frac{q_*}{8\pi^2 l}(q_*{}^2 l\, I_4 - tI_6) + \frac{A^2}{\pi^2 l^2 q_*}(I_9 + 2q_*{}^2 l I_6) \quad (4.9)$$

According to the assumption eq 4.1, ρ reaches a finite value in the limit $l \to \infty$ and the exact expressions (B7)−(B9) for I_4, I_6, and I_9 have to be used. The mean-field values ρ_0 and s_0 for the parameters ρ and s can be found from the equations obtained by inserting the mean-field values of eq 4.7 for A and q_* into F_1 and subsequently minimizing with respect to ρ and s:

$$\frac{\partial F_1(A_0, q_0, \rho, s)}{\partial \rho} = 0 \qquad \frac{\partial F_1(A_0, q_0, \rho, s)}{\partial s} = 0 \quad (4.10)$$

Solving eq 4.10 gives for all microphase-separated structures under consideration

$$\rho_0 = 8A_0\sqrt{2} + 3 - \frac{t}{A_0\sqrt{2}} \qquad s_0 = 2 \quad (4.11)$$

which, after substitution of the expression eq 4.7 for A_0, gives up to the adopted accuracy

$$\rho_0 = \frac{(16-\lambda)t}{6} + 9\mu|\epsilon|\sqrt{2} \qquad s_0 = 2 \quad (4.12)$$

Note that for phases with $\lambda > 16$ (such as the bcc phase) the value of ρ *decreases* with the increasing value of t, meaning that the fluctuations increase. At a certain point the value of ρ approaches zero, which implies that the phase becomes unstable with respect to a phase transition to another phase. To discuss the results obtained, we take as an example the lamellar phase for $f = {}^1/_2$. Then the solutions of eqs 4.7 and 4.12 reduce to

$$A_{\mathrm{lam}} = \frac{t}{3\sqrt{2}} \qquad l q_{\mathrm{lam}}{}^2 = \frac{t}{3} \qquad \rho_{\mathrm{lam}} = t \qquad s_{\mathrm{lam}} = 2 \quad (4.13)$$

satisfying the original assumption eq 4.1 concerning the scaling with l of the adjustable parameters. According to Figure 2, $s = 2$ implies that the system exhibits a residual forward scattering due to the presence of concentration fluctuations on arbitrarily long length scales[36] (in monodisperse incompressible block copolymers such scattering is completely suppressed). The result for q_* is more clear when it is rewritten in terms of the characteristic correlation length $d \equiv 2\pi/q_*$ (for the ordered phases d is just the period of the microstructure):

$$d = \frac{2\pi\sqrt{3}}{\sqrt{(\chi - \chi_s)}} \quad (4.14)$$

which simply corresponds to the temperature dependence of the Cahn−Hilliard wavelength characterizing the pattern of the early stage of spinodal decomposition in the corresponding system of disconnected polydisperse blocks:

$$L_{\mathrm{CH}} = \frac{2\pi\sqrt{2}}{\sqrt{(\chi - \chi_s)}} \quad (4.15)$$

It supports the idea that near the spinodal the thermodynamically stable microphase-separated structure in random copolymers can be regarded as a spinodal decomposition pattern, stabilized due to the presence of the chemical bonds. Finally, the parameter ρ determines (together with s) both the height and the width of the scattering peak; see Figure 2. It follows from eq 4.13 that the peak is high and sharp near the critical point and becomes lower and broader on increased segregation.

Supercooled Disordered Phase. It is instructive to analyze the disordered phase for $t > 0$, $l \to \infty$. Since $\langle\psi\rangle = 0$, the free energy F_{dis} is just the sum of the fluctuation corrections D and D_1. Let the l-scaling of the parameters ρ, q_*, and s characterizing the correlations in the disordered phase be

$$\rho \propto l^{-1} \qquad q_* \propto l^{-1/2} \qquad s \propto l^0 \quad (4.16)$$

Then, up to leading order in l^{-1}, the free energy of the disordered phase is

$$F_{\mathrm{dis}} = \frac{s}{64\pi^2 l^2 \rho} + \frac{s\, q^2}{16\pi^2 l\rho} + \frac{s^{1/2} q^3}{8\pi\rho^{1/2}} - \frac{t s^{1/2} q}{8\pi l \rho^{1/2}} \quad (4.17)$$

Minimization with respect to the adjustable parameters is straigthforward. The resulting equilibrium values of these parameters and the free energy expanded to fourth order in t are given by

$$l q_{\mathrm{dis}}{}^2 = \frac{t}{3} \qquad \rho_{\mathrm{dis}} = \frac{27\, s}{64\pi^2 l t^3} \qquad l F_{\mathrm{dis}} = -\frac{t^3}{27} + \frac{4t^4}{81} \quad (4.18)$$

The fluctuation corrections prevent the instability of the disordered phase. According to eq 4.18 in combination with Figure 2, the peak in the correlation function of the disordered phase becomes higher and sharper the more the system is moving off the spinodal $t = 0$ into the region of stability of the ordered phases, which is just the opposite behavior as that for the ordered phases. As will be shown in the next section, for finite (though large) values of l the above analysis is only valid for t-values satisfying $t \gg l^{-1/4}$, and in this region the scattering peak in the correlation function of the disordered phase stays sharp due to the $l^{-1}t^{-3}$-dependence of ρ.

Remarkably, for $t > 0$ and $l \to \infty$ the free energy of the disordered phase and the free energy of the ordered phases not only have the same l-dependence, but are even equal to leading order in t. Moreover, the free energy of the disordered phase turns out to coincide with the free energy of the random wave structure to fourth order in t. This similarity between the supercooled disordered phase and the random wave structure can be extended even more. Consider the quantity $\int \mathrm{d}\vec{x}\, \langle\psi^2(\vec{x})\rangle$, which is a measure of the amplitude of the concentration inhomogeneities. For all ordered phases it is given by

$$\frac{1}{V}\int \mathrm{d}\vec{x}\, \langle\psi^2(\vec{x})\rangle \cong \frac{1}{V}\int \mathrm{d}x\, \langle\psi(\vec{x})\rangle^2 = \frac{A^2}{k}\sum_{\vec{Q}_1\vec{Q}_2} \frac{1}{V}\int \mathrm{d}x\, \exp(i(\vec{Q}_1 + \vec{Q}_2)\cdot\vec{x}) = 2A^2 \cong \frac{t^2}{9} \quad (4.19)$$

In the first step, use is made of the fact that the ordered phases are not fluctuating in the limit $l \to \infty$ (in fact, $\delta\psi/\psi \propto l^{-1/4}$). For the disordered phase it follows similarly

$$\frac{1}{V}\int \mathrm{d}\vec{x}\ \langle\psi^2(\vec{x})\rangle = \langle\psi^2(\vec{x})\rangle = \langle\psi^2(\vec{x})\rangle - \langle\psi(\vec{x})\rangle^2 = \frac{1}{(2\pi)^3}\int \mathrm{d}\vec{q}\ G(\vec{q}) = \frac{q_*}{8\pi^2}\int_{-\infty}^{\infty} \mathrm{d}p\ p^2\hat{G}(p) = \frac{q_* I_6}{8\pi^2} \cong \frac{s^{1/2}q_*}{8\pi\rho^{1/2}} \cong \frac{t^2}{9} \quad (4.20)$$

where eqs B5 and B14 of Appendix B have been used. Equations 4.19 and 4.20 show that the amplitude of the concentration inhomogeneities in the supercooled disordered state is equal to the amplitude of the concentration inhomogeneities in any of the ordered phases.

5. Fluctuation Corrections to the Phase Diagram

In this section we incorporate the fluctuation corrections for nearly symmetric correlated random copolymers in the vicinity of the order−disorder transition, both for the disordered phase and for the ordered phases. In this region of the phase diagram, the fluctuation corrections are expected to be large. In the mean-field approximation, the order−disorder transition takes place at $t = 0$. Due to the fluctuation corrections, this value is expected[18] to shift upward according to

$$t_{\mathrm{ODT}} \propto l^{-1/4} \quad (5.1)$$

The purpose of this section is the construction of the phase diagram near the critical point, and the determination of the magnitude of the fluctuations in the profiles. In order to be able to do rigorous calculations, we assume that l is large, and in the calculations we take the limit $l \to \infty$. However, there is an important difference with the previous section, where this limit was taken by keeping the point (ϵ, t) *fixed*. If l increases, the fluctuation region shrinks, and the point (ϵ, t) has to move toward the critical point in order to stay in the region of interest. This can be accomplished by taking the limit $l \to \infty$ under fixed values of the *rescaled* parameters $\tilde{t}$ and $\tilde{\epsilon}$, which are defined by

$$\tilde{t} \equiv l^{1/4}t \qquad \tilde{\epsilon} = l^{1/4}\epsilon \quad (5.2)$$

In parallel with the analysis given in section 4, we assume scaling laws for the adjustable parameters A, q_*, ρ and s that will be verified by the fact that the subsequent calculations result in explicit expressions for these parameters satisfying these laws. However, in the region considered now, these scaling laws are different from eq 4.1, namely:

$$\rho \propto l^{-1/4} \qquad s \propto l^0$$

$$A \propto t \propto l^{-1/4} \qquad {q_*}^2 \propto \chi - \chi_s \equiv \frac{t}{l} \propto l^{-5/8} \quad (5.3)$$

Disordered Phase. For nearly symmetric correlated random copolymers close to the order−disorder transition, the free energy F^{dis} of the disordered phase can be written as a power series in $l^{-1/8}$:

$$F_{\mathrm{dis}} = F_0^{\mathrm{dis}} + F_1^{\mathrm{dis}} + F_2^{\mathrm{dis}}$$

$$F_0^{\mathrm{dis}} \propto l^{-14/8} \qquad F_1^{\mathrm{dis}} \propto l^{-15/8} \qquad F_2^{\mathrm{dis}} \propto l^{-16/8} \quad (5.4)$$

To keep all these terms is necessary since, as will be shown below, the free energies of the disordered phase and the various ordered phases turn out to differ only by the terms of the order $l^{-16/8}$. The only contributions to F^{dis} are D and D_1. Since ρ approaches zero when l approaches infinity (eq 5.3), it is justified to use the expansion of the diagrams in powers of ρ (see Appendices A and B)

$$F_0^{\mathrm{dis}} = \frac{s}{64\pi^2 l^2\rho} + \frac{{q_*}^3 s^{1/2}}{8\pi\rho^{1/2}} - \frac{q_* t\, s^{1/2}}{8\pi l\rho^{1/2}} \quad (5.5)$$

In order to make the l-dependence of the parameters explicit, it is convenient to define rescaled parameters $\tilde{x}$, $\tilde{q}$, and $\tilde{\rho}$, which reach a finite limit for $l \to \infty$, as follows

$$\tilde{\rho} = l^{1/4}\rho \qquad \tilde{x} = \frac{s^{1/2}}{8\pi\tilde{\rho}^{1/2}} \qquad \tilde{q} = l^{5/8}q_* \quad (5.6)$$

In terms of these quantities, the expression for F_0 simplifies to

$$F_0^{\mathrm{dis}} = \frac{1}{l^{14/8}}(\tilde{x}^2 + \tilde{q}^3\tilde{x} - \tilde{q}\tilde{t}\tilde{x}) \quad (5.7)$$

Minimization with respect to $\tilde{q}$ and $\tilde{x}$ yields

$$\tilde{q}^2 = \frac{\tilde{t}}{3} \qquad \tilde{x} = \tilde{q}^3 \quad (5.8)$$

$$F_0^{\mathrm{dis}} = -\frac{\tilde{t}^3}{27\, l^{14/8}} \quad (5.9)$$

The second contribution F_1^{dis} is proportional to $l^{-15/8}$. Using the expressions given in Appendices A and B one obtains

$$F_1^{\mathrm{dis}} = \frac{1}{8\pi l^{15/8}}\left((1-s)\tilde{x} + \frac{\tilde{x}}{s} + \frac{(s-1)\tilde{x}}{s} + \frac{2\tilde{q}^3(s-1)^{3/2}}{3}\right) \quad (5.10)$$

After substitution of the solution eq 5.8 for $\tilde{x}$, this rearranges to

$$F_1^{\mathrm{dis}} = \frac{\tilde{q}^3}{8\pi l^{15/8}}\left(2 - s + \frac{2(s-1)^{3/2}}{3}\right) \quad (5.11)$$

Minimization with respect to s gives

$$s = 2 \qquad F_1^{\mathrm{dis}} = \frac{\tilde{t}^{3/2}}{36\pi\sqrt{3}l^{15/8}} \quad (5.12)$$

Since up to this order the free energies of the disordered phase and the ordered phases will turn out to be equal, it is necessary to calculate F_2^{dis} as well, containing the terms proportional to $l^{-16/8}$. There are two contributions. The first one, F_{2a}^{dis}, consists just of those terms in the expansion of D and D_1 that have the proper

scaling with l. Substituting the results for s, $\tilde{q}$, and $\tilde{x}$ gives

$$F_{2a}^{dis} = \frac{1}{l^2}\left(\frac{7}{128\pi^2} + \frac{4\tilde{t}^4}{81}\right) \tag{5.13}$$

The second contribution F_{2b}^{dis} arises from the fact that the equilibrium values of eqs 5.8 and 5.12 for the parameters s, $\tilde{q}$, and $\tilde{x}$ providing the minimum of the isolated terms of eqs 5.7 and 5.11 should be corrected to give the minimum of their sum in eq 5.4, the magnitude of the correction as compared to the major contribution being of the order $l^{-1/8}$. The effect of this discrepancy is

$$F_2^{dis} = -\frac{1}{2}\frac{\partial F_1^{dis}}{\partial x_i}\left(\frac{\partial^2 F_0^{dis}}{\partial x_i \partial x_j}\right)^{-1}\frac{\partial F_1^{dis}}{\partial x_j} = -\frac{1}{192\pi^2 l^2} \tag{5.14}$$

with $x_1 = s$, $x_2 = \tilde{q}$, $x_3 = \tilde{x}$. Summarizing, the equilibrium values of the rescaled parameters in eq 5.6 for the disordered phase are finite (which verifies the assumption in eq 5.3 concerning their l-scaling) and given by

$$s_{dis} = 2 \qquad \tilde{\rho}_{dis} = \frac{27}{32\pi^2\tilde{t}^3} \qquad \tilde{q}_{dis}{}^2 = \frac{\tilde{t}}{3} \tag{5.15}$$

and the complete $\tilde{t}$-dependence of F^{dis} is given by

$$F^{dis} = -\frac{\tilde{t}^3}{27 l^{14/8}} + \frac{\tilde{t}^{3/2}}{36\pi\sqrt{3} l^{15/8}} + \frac{19}{384\pi^2 l^2} + \frac{4\tilde{t}^4}{81 l^2} \tag{5.16}$$

Lamellar Phase. The free energy of the *ordered phases* contains the mean-field contribution F_L as well as the fluctuation corrections D, D_1, and D_2 (see Appendices A and B). We assume that, for the parameters q_*, s, and ρ of the lamellar phase, the scaling laws given in eq 5.3 hold. Then F^{lam} may be expanded in powers of $l^{-1/8}$:

$$F^{lam} = F_0^{lam} + F_1^{lam} + F_2^{lam}$$
$$F_0^{lam} \propto l^{-14/8} \qquad F_1^{lam} \propto l^{-15/8} \qquad F_2^{lam} \propto l^{-16/8} \tag{5.17}$$

The minimization with respect to the amplitude A is straightforward. The free energy contains terms proportional to A^2, arising from the mean-field contribution F_L and the fluctuation correction D_2 and terms proportional to A^4 arising from F_L. Very important is the sign of the quadratic coefficient. If it is positive, minimization with respect to A leads to $A = 0$, which returns to the analysis for the disordered phase. In the following it will be assumed that it is negative, leading to a nonzero value for A. Afterward it will be verified under which conditions this assumption is correct. To leading order in l, this coefficient (we will refer to it as τ_{eff}) is given by

$$\tau_{eff} = \left(2(\tilde{q}^2 - \tilde{t}) + \frac{s^{1/2}}{2\pi\tilde{q}\tilde{\rho}^{1/2}}\right) l^{-5/4} \tag{5.18}$$

Under the assumption that eq 5.18 is negative, the minimization with respect to A is straightforward and leads to

$$F_0^{lam} = -\frac{\tilde{q}^2(\tilde{t} - \tilde{q}^2)^2}{4 l^{14/8}} \tag{5.19}$$

$$F_1^{lam} = \frac{\tilde{q}(\tilde{q}^2(-6 + 4(s-1)^{3/2} + 3s) + 3\tilde{t}(2 - s))}{48\pi l^{15/8}} \tag{5.20}$$

$$F_2^{lam} = \frac{5\tilde{q}^4(\tilde{t} - \tilde{q}^2)^2}{8 l^2} + \frac{2\pi - 8s + 4\pi s + 4s^2 - \pi s^2}{256\pi^3 l^2} - \frac{3\, s\tilde{q}^2}{128\pi^2 l^2 \tilde{\rho}} + \frac{3\tilde{q}^3 s^{1/2}(\tilde{t} - \tilde{q}^2)}{16\pi l^2 \tilde{\rho}^{1/2}} + \frac{\tilde{q} s^{1/2}(-\tilde{q}^2 - 2s\tilde{q}^2 + 3\tilde{t})\tilde{\rho}^{1/2}}{32\pi l^2} \tag{5.21}$$

Note that F_0 depends only on $\tilde{q}$, F_1 depends on both $\tilde{q}$ and s, and F_2 depends on all three parameters $\tilde{q}$, s, and $\tilde{\rho}$. This fact simplifies the minimization procedure. Since F_0 is the dominant contribution to the free energy, the value of $\tilde{q}$ will be determined by F_0. Minimization of F_0 with respect to $\tilde{q}$ leads to

$$\tilde{q}_{lam}{}^2 = \frac{\tilde{t}}{3} \qquad F_0^{lam} = -\frac{\tilde{t}^3}{27 l^{14/8}} \tag{5.22}$$

which is the same result as for the disordered phase, eqs 5.8 and 5.9. Inserting this value for $\tilde{q}$ into the expression for F_1^{lam} and then minimizing with respect to s give

$$s_{lam} = 2 \qquad F_1^{lam} = \frac{\tilde{t}^{3/2}}{36\pi\sqrt{3} l^{15/8}} \tag{5.23}$$

again the same result as for the disordered phase given in eq 5.12, which is the reason the terms proportional to l^{-2} have to be calculated as well. Now there are three contributions. The first one is calculated by inserting the expressions for $\tilde{q}$ and s (eqs 5.22 and 5.23) into the first two terms of eq 5.21:

$$F_{2a}^{lam} = \frac{5\tilde{t}^4}{162 l^2} + \frac{3}{128\pi^2 l^2} \tag{5.24}$$

The second one is (see the comment above eq 5.14)

$$F_{2b}^{lam} = -\frac{1}{2}\sum_{i,j}\frac{\partial F_1^{lam}}{\partial x_i}\left(\frac{\partial^2 F_0^{lam}}{\partial x_i \partial x_j}\right)^{-1}\frac{\partial F_1^{lam}}{\partial x_j} = -\frac{1}{192\pi^2 l^2} \tag{5.25}$$

The third contribution results from the $\tilde{\rho}$-dependent terms in eq 5.21. With the expressions for $\tilde{q}$ and for s (eqs 5.22 and 5.23), this contribution is

$$F_{2c}^{lam} = \frac{\tilde{t}}{12\sqrt{6} l^2 \pi}\left(-\frac{3\sqrt{6}}{16\pi}\frac{1}{\tilde{\rho}} + \frac{\tilde{t}^{3/2}}{\tilde{\rho}^{1/2}} + \tilde{t}^{1/2}\tilde{\rho}^{1/2}\right) \tag{5.26}$$

Collecting all the terms, the total free energy F^{lam} is

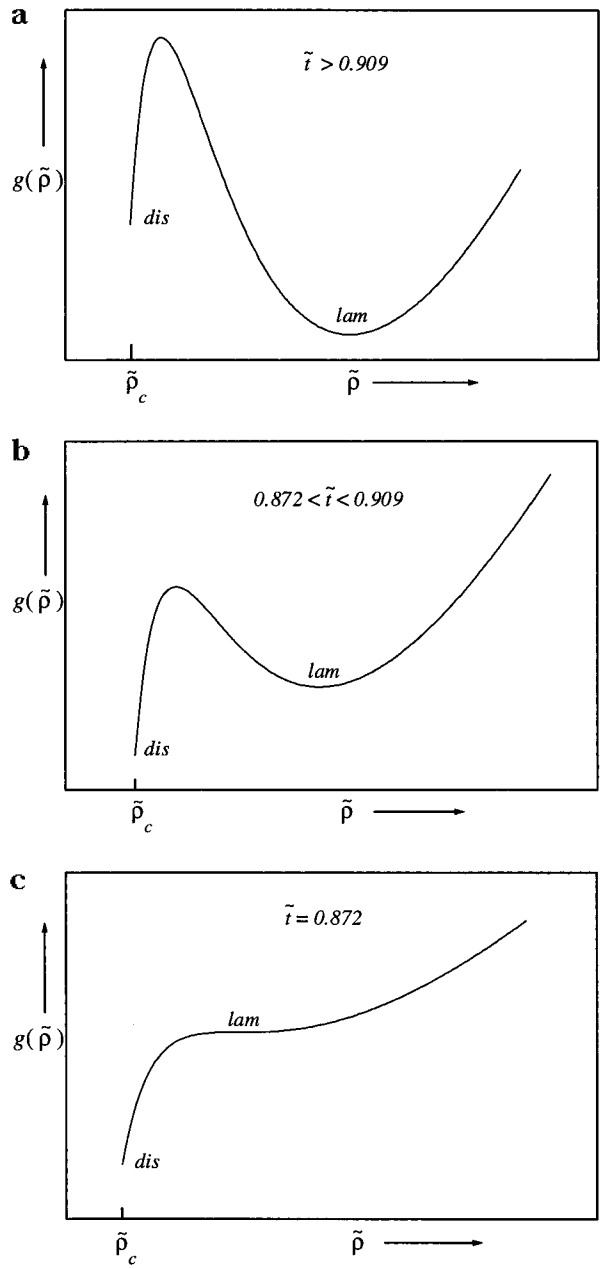

Figure 3. Dependence of the free energy of the lamellar phase (*lam*) on the value of the parameter $\tilde{\rho}$ for three distinct values of the rescaled interaction $\tilde{t}$. The free energy of the disordered phase is indicated as well (*dis*). (a) The lamellar phase is completely stable. (b) The lamellar phase is metastable. (c) The lamellar phase loses stability.

obtained as a function of $\tilde{t}$ and $\tilde{\rho}$

$$F^{\text{lam}} = -\frac{\tilde{t}^3}{27l^{14/8}} + \frac{\tilde{t}^{3/2}}{36\pi\sqrt{3}l^{15/8}} + \frac{5\tilde{t}^4}{162l^2} + \frac{7}{384\pi^2 l^2} + \frac{\tilde{t}g(\tilde{\rho})}{12\sqrt{6}l^2\pi}$$

$$g(\tilde{\rho}) = -\frac{3\sqrt{6}}{16\pi}\frac{1}{\tilde{\rho}} + \frac{\tilde{t}^{3/2}}{\tilde{\rho}^{1/2}} + \tilde{t}^{1/2}\tilde{\rho}^{1/2} \qquad (5.27)$$

This expression still has to be minimized with respect to $\tilde{\rho}$. It is important to note that the domain of definition of the function $g(\tilde{\rho})$ is bounded by the condition

$$\tau_{\text{eff}} \le 0 \qquad (5.28)$$

necessary to have a nonzero equilibrium value of the amplitude A. Using eq 5.18 for τ_{eff} together with the values of s_{lam} and q_{lam} shows that this condition is equivalent to

$$\tau_{\text{eff}} \le 0 \Leftrightarrow \tilde{\rho} \ge \frac{27}{32\pi^2\tilde{t}^3} = \tilde{\rho}_{\text{dis}} \qquad (5.29)$$

In Figure 3, the function $g(\tilde{\rho})$ given in eq 5.27 is shown for three values of $\tilde{t}$. The point on the curve corresponding to the disordered phase is marked *dis*, whereas the point corresponding to the lamellar phase is marked *lam*. In Figure 3a the lamellar phase is stable, in Figure 3b it is metastable, and in Figure 3c it loses stability. The values of $\tilde{t}$ for which this happens can easily be extracted from eq 5.27. Going back from $\tilde{t}$ to the original parameter χ, the results can be summarized as follows:

$\chi - \chi_c > 0.909l^{-5/4}$ the lamellar phase is stable

$0.909l^{-5/4} > \chi - \chi_c > 0.872l^{-5/4}$ the lamellar phase is metastable

$\chi - \chi_c = 0.872l^{-5/4}$ the lamellar phase loses stability

In order to show that everywhere in the phase diagram the disordered phase is at least metastable, we calculate the slope of the function $g(\tilde{\rho})$ at the point $\tilde{\rho} = \tilde{\rho}_{\text{dis}}$:

$$\left.\frac{dg(\tilde{\rho})}{d\tilde{\rho}}\right|_{\tilde{\rho}=\tilde{\rho}_c} = \frac{2\pi\tilde{t}^2\sqrt{2}}{3\sqrt{3}} > 0 \qquad (5.30)$$

Since this is positive for all values of $\tilde{t}$, there is always an energy barrier between the disordered state and the lamellar state, which proves our assertion. For the range of $\tilde{t}$-values $\tilde{t} > 0.872$ for which the lamellar phase is (meta-)stable, the $\tilde{\rho}$-dependent part $g(\tilde{\rho})$ of the free energy in eq 5.27 can be minimized rigorously. The result is

$$F^{\text{lam}} = -\frac{\tilde{t}^3}{27l^{14/8}} + \frac{\tilde{t}^{3/2}}{36\pi\sqrt{3}l^{15/8}} + \frac{7}{384\pi^2 l^2} + \frac{5t^4}{162l^2} + \frac{\tilde{t}^2}{24\pi\sqrt{6}l^2}\left(J + \frac{1}{J}\right)$$

$$q_*{}^2 = \frac{t}{3l} \qquad s = 2 \qquad \rho = \frac{tJ^2}{3}$$

$$J = 2\cos\left[\frac{\pi}{3} - \frac{1}{3}\arctan\sqrt{\frac{128\pi^2\tilde{t}^4}{729} - 1}\right] \quad \tilde{t} > 0.872 \qquad (5.31)$$

For large values of $\tilde{t}$ the expression for ρ simplifies to

$$\rho \to \frac{4t}{3}\cos^2\left[\frac{\pi}{3} - \frac{1}{3}\frac{\pi}{2}\right] = t \qquad (5.32)$$

which coincides with the mean-field value derived in section 4, eq 4.13.

Structures Other Than Lamellar. In order to calculate the free energy for other microstructures, note that they can be expanded in powers of $l^{-1/8}$ as well:

$$F = F_0 + F_1 + F_2$$

$$F_0 \propto l^{-14/8} \qquad F_1 \propto l^{-15/8} \qquad F_2 \propto l^{-16/8} \quad (5.33)$$

After minimization with respect to the amplitude A, the expressions for F_0 and F_1 prove to be independent of the type of structure and are given by eqs 5.22 and 5.23, respectively. Therefore, the parameters q_* and s determined by the minimization of F_0 and F_1, respectively, have the same values for all structures (to leading order in l). Thus, the differences in the free energies of the various structures are completely due to F_2. Inserting the values for q_* and s, one obtains F_2 as a function of $\tilde{\rho}$ for general values of μ and λ.

$$l^2F_2 = \frac{7}{384\pi^2} + (\lambda - 16)\left(\frac{\tilde{t}}{384\pi^2\tilde{\rho}} - \frac{\tilde{t}^{5/2}}{72\sqrt{6}\pi\tilde{\rho}^{1/2}}\right) + \frac{\tilde{t}^{3/2}\tilde{\rho}^{1/2}}{12\sqrt{6}\pi} + \frac{\lambda\tilde{t}^4}{324} - 24\mu|\tilde{\epsilon}|A_0^3(\tilde{\rho})$$

$$A_0(\tilde{\rho}) = \left(\frac{\tilde{t}^2}{18} - \frac{\tilde{t}^{1/2}}{8\sqrt{6}\pi\tilde{\rho}^{1/2}}\right)^{1/2} \quad (5.34)$$

where $A_0(\tilde{\rho})$ is the equilibrium amplitude value given a fixed value for the parameter $\tilde{\rho}$. Remarkably, for the random wave structure, which has $\mu = 0$ and $\lambda = 16$, the second and fifth term on the right hand side vanish and the only $\tilde{\rho}$-dependence comes from the third term. Therefore, for the random wave structure, the free energy decreases continuously with a decrease of $\tilde{\rho}$ to the lower bound of its domain of definition eq 5.28. At that point, the amplitude A is zero, and the values of the free energy and of the parameters $\tilde{\rho}$, s, and q_* coincide with those for the disordered phase, eqs 5.15 and 5.16. We can conclude that the random wave structure is completely unstable with respect to a transition to the disordered phase (so it is not even metastable).

For general values of μ and λ, F_2 as given by eq 5.34 must be minimized with respect to $\tilde{\rho}$. In order to construct the phase diagram in the plane $\tilde{t} = l^{1/4}(l\chi - 1)$ versus $\tilde{\epsilon} = l^{1/4}(f - 1/2)$, the minimum values of F_2 are calculated numerically and compared for the various ordered structures, which results in the phase diagram shown in Figure 4. To visualize the fluctuation corrections better, the mean-field phase transition lines *lam/cyl* and *cyl/bcc* are presented in the same figure by dashed lines.

As can be seen from the phase diagram, the larger the distance to the critical point, the closer the phase transition lines are to their mean-field approximations. For the phase transition lines between the various ordered phases, the fluctuation corrections decay much faster than for the transitions from the disordered phase into an ordered phase. It is worthwhile to note also that for the correlated random copolymers the "windows" where the disorder-order transition occurs into the lamellar or hexagonal phase (respectively for $|\tilde{\epsilon}| < 0.0624$ and $0.0624 < |\tilde{\epsilon}| < 0.133$) are fairly small when compared with the corresponding windows found in ref 23 for the monodisperse diblock copolymers.

Fluctuations in the Profiles near the ODT. Although for the construction of the phase diagram shown in Figure 4 the fluctuation corrections have been taken into account, this phase diagram shows only the

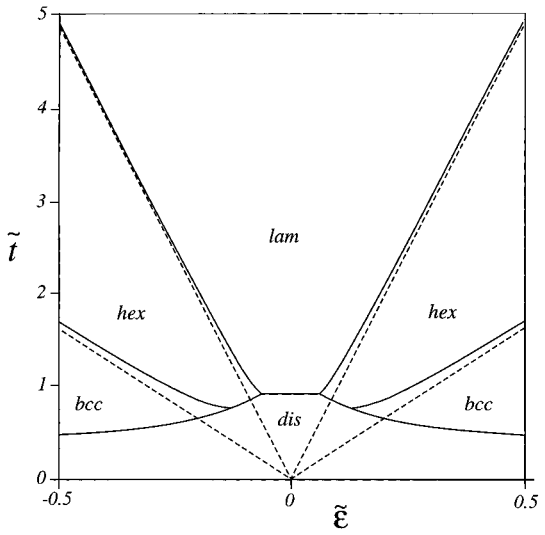

Figure 4. Phase diagram for a correlated random copolymer melt in the vicinity of the critical point $f_c = 1/2$, $\chi_c = 1/l$ taking the fluctuation corrections into account. Horizontal: rescaled A-monomer fraction $\tilde{\epsilon} \equiv l^{1/4}(f - 1/2)$. Vertical: rescaled interaction strength $\tilde{t} \equiv l^{5/4}(\chi - \chi_c)$. Dashed lines are mean-field boundaries.

average profiles $\langle\psi\rangle$. Due to the presence of the fluctuations, the *instantaneous* profile ψ is different from the average profile. The difference between these profiles is largest in the vicinity of the critical point. In order to get an idea about the magnitude of the fluctuations, we calculate, for $f = 1/2$ at the phase transition point $\tilde{t} = 0.909$, the quantity $\langle\psi^2\rangle$ both in the lamellar phase and in the disordered phase. Note that $\langle\psi^2\rangle$ includes automatically the contribution from the fluctuations. For the lamellar phase we have

$$\langle\psi^2\rangle_{\text{lam}} \equiv \frac{1}{V}\int \mathrm{d}\vec{x}\,\langle\psi^2(\vec{x})\rangle = \frac{1}{V}\int \mathrm{d}\vec{x}\,(\langle\psi^2(\vec{x})\rangle - \langle\psi(\vec{x})\rangle^2 + \langle\psi(\vec{x})\rangle^2)$$

$$= \frac{1}{(2\pi)^3}\int \mathrm{d}\vec{q}\; G(\vec{q}) + \frac{1}{V}\int \mathrm{d}\vec{x}\,\langle\psi(\vec{x})\rangle^2 = \frac{s^{1/2}q_*}{8\pi\rho^{1/2}} + 2A^2\Big|_{\tilde{t}=0.909}$$

$$= (0.046 + 0.046)l^{-1/2} \quad (5.35)$$

The first contribution is due to the fluctuations, and the second contribution is due to the average profile. Since these contributions are equal, the amplitude of the fluctuations $\delta\psi$ in the profile is equal to the amplitude of the average profile $\langle\psi\rangle$. This implies that the profile is strongly fluctuating and rather irregular. For the disordered phase the corresponding result is

$$\langle\psi^2\rangle_{\text{dis}} = \langle\psi^2(\vec{x})\rangle = \frac{1}{(2\pi)^3}\int \mathrm{d}\vec{q}\; G(\vec{q}) = \frac{s^{1/2}q_*}{8\pi\rho^{1/2}}\Big|_{\tilde{t}=0.909} = 0.092l^{-1/2} \quad (5.36)$$

Comparing eq 5.35 with eq 5.36 shows that, for $f \cong 1/2$ at the ODT, the amplitude of the concentration inhomogeneities in the disordered phase is equal to the amplitude of the concentration inhomogeneities in the

ordered phase (it was shown in section 4 that this remains true for stronger segregations, but then the disordered phase is metastable). Therefore, the disordered phase is far from homogeneous. We can conclude that in this region of the phase diagram the various phases look similar. This suggests that near the ODT the disordered phase has the appearance of a disordered microphase-separated structure (the random wave structure, which is, however, itself unstable). This similarity is confirmed also by the properties of the correlation function in the disordered phase. In eq 3.18 an expression was obtained for the correlation function $G(\vec{x})$ in real space. $G(\vec{x})$ is an exponentially decaying sine, characterized by two length scales: the period R_{osc} of the oscillations and the correlation length R_{cor}. In the disordered phase near the ODT, the values of s and ρ satisfy $s = 2$ and $\rho \propto l^{-1/4} \ll 1$ (eq 5.3). Inserting this into eq 3.19 leads to $a \cong 1$, $b \cong \sqrt{\rho/2} \ll 1$, and so

$$R_{cor} \gg R_{osc} \tag{5.37}$$

Therefore, the correlation function exhibits a large number of oscillations before it vanishes, which means that *locally* the disordered phase appears to have some kind of ordering (see also ref 12, where the same result was obtained for a melt of *un*correlated random copolymers).

6. Concluding Remarks

Summarizing, a quantitative theory has been presented for the phase behavior of correlated random copolymer melts with due regard for the fluctuation corrections. By doing so, it was shown that the order−disorder transition occurs into thermodynamically stable microstructures having the conventional bcc, cylindrical, and lamellar symmetry and that the so-called random wave structure (a nonperiodic microstructure) is unstable; see Figure 4. The almost symmetric correlated random copolymer was shown to undergo a direct phase transition from the disordered phase to the lamellar or the cylindrical phase. The width Δf of the corresponding sections of the phase transition line decreases with increasing block length l as $\Delta f \propto l^{-1/4}$.

For the interpretation of the phase diagram Figure 4 it is important to realize that it gives only information about the *average* profiles, whereas the *instantaneous* profiles will be rather different due to the fluctuations. For instance, for $f = 1/2$ at the order−disorder transition, all phases are strongly fluctuating: in the ordered phases the amplitude of the fluctuations equals the amplitude of the average profile, and in the disordered phase the concentration inhomogeneities have the same amplitude as those in the ordered phases. This similarity between the disordered phase and the ordered phases (especially the random wave structure) in this region of the phase diagram is also confirmed by the fact that the disordered phase has an anomalously large correlation length, giving the phase a kind of local ordering.[12,37] In connection with this it is interesting to note that for $t > 0$ in the limit $l \to \infty$ the free energy of the random wave structure coincides with the free energy of the disordered phase. However, it should be born in mind that strictly speaking these phases are different: $\langle\psi\rangle = 0$ for the disordered phase, whereas $\langle\psi\rangle \neq 0$ for the random wave structure. Moreover, it follows from eq 5.34 that the random wave structure is completely unstable (at least within the approximation used in this paper). Since for correlated random copolymer melts the fluctuation corrections are considerable even for rather large values of the chemical correlation length l, we suspect that the experimentally observed disordered structure in random copolymers is in fact a strongly fluctuating disordered phase.[37]

The last point to be discussed is related to the fundamental notion of thermodynamic equilibrium in the system under investigation. In this paper, the procedure to construct the phase diagram implies that the system remains in a single phase, and the possibility of separation into coexisting phases was neglected. However, it follows from the Hamiltonian[25,26] eq 3.5 that the phase diagram given complete thermodynamic equilibrium contains certain *two-phase strips* separating the one-phase regions. This was shown by straightforward calculation for a polydisperse diblock copolymer melt in ref 27 (see also ref 31). Allowing for the possibility of macrophase separation into coexisting phases could be important, and for the correlated random copolymer its effect can be calculated, for instance, via straightforward application of the Panyukov−Kuchanov methods[32,33] or by making use of the detailed densities theory.[27,34] In the mean-field approximation these strips were shown to be rather narrow, except for the transition from the disordered state.[33] However, even if the conditions are such that the true equilibrium corresponds to the situation where the system is separated into coexisting phases, the polymer chains must diffuse over macroscopic distances in order to achieve this situation. As was shown recently,[35] the diffusion time τ_{dif} in random copolymer systems scales with the molecule length N like $\tau_{dif} \propto \exp[\sqrt{N}]$. Therefore, since we considered the system in the limit $N \to \infty$, it would take an infinite amount of time for the system to reach equilibrium. In order to reach a microphase-separated state, it is *not* necessary for the chains to diffuse as a whole, since a local adaptation of their conformations will be sufficient. In conclusion, we can say that for experimental random copolymer systems, perfect thermodynamic equilibrium might never be reached, and the phase diagram shown in Figure 4 represents what is going on in real systems, notwithstanding the fact that in some parts of the (f, χ) plane it only gives a *meta*stable state. A more detailed discussion of this problem will be given elsewhere.[34]

Acknowledgment. We thank the referees for the helpful comments enabling us to improve the paper.

Appendix A

In this appendix the fluctuation corrections to the free energy, given in eqs 3.13 and 3.14, are calculated using the trial functions eq 3.15 for the concentration profile ψ and eq 3.17 for the correlation function G. It is convenient to rewrite eq 3.17 as follows:

$$\hat{G}(p) = \frac{p^2 + s - 1}{((p-a)^2 + b^2)((p+a)^2 + b^2)} \tag{A1}$$

$$a = \frac{\sqrt{1 - \rho/2 + \sqrt{1 - \rho + \rho s}}}{\sqrt{2}}$$

$$b = \frac{\sqrt{-1 + \rho/2 + \sqrt{1 - \rho + \rho s}}}{\sqrt{2}} \tag{A2}$$

Rewrite eq 3.14a as $D_1 = D_1^a + D_1^b$, where

$$D_1^a \equiv \frac{1}{128\pi^6 l^2}\int \mathrm{d}\vec{p}_1\,\mathrm{d}\vec{p}_2\,\frac{\widehat{G}(\vec{p}_1)\,\widehat{G}(\vec{p}_2)}{{p_1}^2+{p_2}^2}$$

$$= \frac{1}{64\pi^5 l^2}\int \mathrm{d}\vec{p}\;\widehat{G}(p)\frac{\pi(s-1+2yp+\sqrt{1-\rho+\rho s})}{2b((p+b)^2+a^2)}$$

$$= \frac{1}{32\pi^3 l^2 b}\int_0^\infty \mathrm{d}p\;\times \frac{p^2(p^2+s-1)(s-1+2yp+\sqrt{1-\rho+\rho s})}{((p-a)^2+b^2)((p+a)^2+b^2)((p+b)^2+a^2)}$$

$$= \frac{I_3}{32\pi^3 l^2}+\frac{I_1}{16\pi^3 l^2}+\frac{(s-1)I_2}{16\pi^3 l^2} \tag{A3}$$

For the definition and the evaluation of the integrals I_1, I_2, and I_3, the reader is referred to Appendix B. The second contribution D_1^b to D_1 is

$$D_1^b = \frac{{q_*}^2}{16\pi^4 l}\left(\int_{-\infty}^{\infty}\mathrm{d}p\;p^2\widehat{G}(p)\right)^2 = \frac{{q_*}^2 {I_6}^2}{16\pi^4 l} \tag{A4}$$

For D_2, defined in eq 3.14b, the result is $D_2 = D_2^a + D_2^b$, where

$$D_2^a = \frac{A^2}{\pi^2 l^2 q_*}\int_{-\infty}^{\infty}\mathrm{d}p\;\frac{p^2\widehat{G}(p)}{1+p^2} = \frac{A^2}{\pi^2 l^2 q_*}\,I_9 \tag{A5}$$

$$D_2^b = \frac{2A^2 q_*}{\pi^2 l}\,I_6 \tag{A6}$$

Finally, the contribution D has to be calculated:

$$D = \frac{1}{2V}\int \mathrm{d}\vec{x}_1\,d\vec{x}_2\,\Gamma_2(\vec{x}_1,\vec{x}_2)\,G(\vec{x}_1,\vec{x}_2) - \frac{1}{V}\,\mathrm{Tr}\ln G(\vec{x}_1,\vec{x}_2)$$

$$= \frac{1}{2}\frac{1}{(2\pi)^3}\int_{-\infty}^{\infty}\mathrm{d}q\;2\pi q^2\,(\Gamma_2(q)\,G(q)-\ln G(q)) \tag{A7}$$

For the calculation of the trace, see ref 24. One obtains

$$D = \frac{1}{2}\frac{1}{(2\pi)^2}\int_{-\infty}^{\infty}\mathrm{d}q\;q^2(2q^2G(q)-\ln G(q)) - \frac{1}{2}\frac{1}{(2\pi)^2}\frac{t}{l}\int_{-\infty}^{\infty}\mathrm{d}q\;q^2G(q) \tag{A8}$$

Both integrals in eq A8 are divergent. However, these divergencies can be removed by adding functions to the integrands that do not depend on the parameters A, q_*, ρ, and s.

$$D = \frac{1}{2}\frac{1}{(2\pi)^2}\int_{-\infty}^{\infty}\mathrm{d}q\;q^2[2q^2G(q)-1-\ln(2q^2G(q))] - \frac{1}{2}\frac{1}{(2\pi)^2}\frac{t}{l}\int_{-\infty}^{\infty}\mathrm{d}q\;q^2\left[G(q)-\frac{1}{2q^2}\right]$$

$$= \frac{1}{2}\frac{{q_*}^3}{(2\pi)^2}\int_{-\infty}^{\infty}\mathrm{d}p\;p^2(p^2\widehat{G}(p)-1-\ln p^2\widehat{G}(q)) - \frac{1}{(2\pi)^2}\frac{t}{l}\frac{q_*}{2}\int_{-\infty}^{\infty}\mathrm{d}p\;p^2\left(\widehat{G}(p)-\frac{1}{p^2}\right)$$

$$= \frac{{q_*}^3}{8\pi^2}I_4 - \frac{tq_*}{8\pi^2 l}I_6 \tag{A9}$$

Appendix B.

In this appendix the expressions for the integrals I_1, I_2, I_3, I_4, I_6, and I_9 used in Appendix A are given. These integrals are defined by

$$I_1 = \int_0^\infty \mathrm{d}p\,\frac{p^5}{((p-a)^2+b^2)((p+a)^2+b^2)((p+b)^2+a^2)} \tag{B1}$$

$$I_2 = \int_0^\infty \mathrm{d}p\,\frac{p^3}{((p-a)^2+b^2)((p+a)^2+b^2)((p+b)^2+a^2)} \tag{B2}$$

$$I_3 = \frac{1}{b}\int_0^\infty \mathrm{d}p\,\frac{p^2(p^2+s-1)(s-1+\sqrt{1-\rho+\rho s})}{((p-a)^2+b^2)((p+a)^2+b^2)((p+b)^2+a^2)} \tag{B3}$$

$$I_4 = \int_{-\infty}^{\infty}\mathrm{d}p\;p^2(p^2\widehat{G}(p)-1-\ln p^2\widehat{G}(p)) \tag{B4}$$

$$I_6 = \int_{-\infty}^{\infty}\mathrm{d}p\;p^2\widehat{G}(p) \tag{B5}$$

$$I_9 = \int_{-\infty}^{\infty}\mathrm{d}p\,\frac{p^2\widehat{G}(p)}{1+p^2} \tag{B6}$$

The integrals I_6 and I_1 are not convergent; however, their derivatives with respect to ρ and s are convergent. The procedure is to calculate these derivatives and, afterward integrate them, which comes down to substracting an infinite constant. In section 4, exact expressions for I_4, I_6, and I_9 are needed:

$$\frac{I_4}{\pi} = \frac{2(s-1)^{3/2}}{3} + \frac{-1-2\rho+\rho^2+6s-2\rho s+(1+\rho-3s)\sqrt{1-\rho+\rho s}}{3\sqrt{2}\sqrt{-1+\rho/2+\sqrt{1-\rho+\rho s}}} \tag{B7}$$

$$\frac{I_6}{\pi} = \frac{1-\rho+s-\sqrt{1-\rho+\rho s}}{\sqrt{2}\,\sqrt{-1+\rho/2+\sqrt{1-\rho+\rho s}}} \tag{B8}$$

$$\frac{I_9}{\pi} = \frac{1+\dfrac{s-2}{1+\sqrt{1-\rho+\rho s}+\sqrt{2}\sqrt{-1+\rho/2+\sqrt{1-\rho+\rho s}}}}{\sqrt{2}\sqrt{-1+\rho/2+\sqrt{1-\rho+\rho s}}} \tag{B9}$$

In section 5 we need the diagrams only in the limit $\rho \to 0$, so it is sufficient to give the Taylor expansion of the

integrals in powers of ρ. The integrals I_1, I_2, and I_3 have to be expanded till order zero, whereas I_4, I_6, and I_9 have to be expanded till order one-half:

$$\frac{I_1}{\pi} = \frac{1}{4s^{1/2}\rho^{1/2}} + \frac{\pi - 1}{4\pi} + O(\rho^{1/2}) \quad \text{(B10)}$$

$$\frac{I_2}{\pi} = \frac{1}{4s^{1/2}\rho^{1/2}} - \frac{\pi + 2}{8\pi} + O(\rho^{1/2}) \quad \text{(B11)}$$

$$\frac{I_3}{\pi} = \frac{s}{2\rho} + \frac{(1 - s)\, s^{1/2}}{2\rho^{1/2}} + \frac{(s - 1)(3\pi + 4s + \pi s)}{8\pi} + O(\rho^{1/2}) \quad \text{(B12)}$$

$$\frac{I_4}{\pi} = \frac{s^{1/2}}{\rho^{1/2}} + \frac{2(s - 1)^{3/2}}{3} - \frac{3 + 2s + 3\, s^2}{8s^{1/2}}\rho^{1/2} + O(\rho) \quad \text{(B13)}$$

$$\frac{I_6}{\pi} = \frac{s^{1/2}}{\rho^{1/2}} + \frac{-3 - 6\, s + s^2}{8s^{1/2}}\rho^{1/2} + O(\rho^{3/2}) \quad \text{(B14)}$$

$$\frac{I_9}{\pi} = \frac{s^{1/2}}{2\rho^{1/2}} + \frac{2 - s}{4} + \frac{s^2 - 3}{16s^{1/2}}\rho^{1/2} + O(\rho) \quad \text{(B15)}$$

References and Notes

(1) Flory, P. J. *Principles of Polymer Chemistry*; Cornell University Press: Ithaca, NY, 1953.
(2) De Gennes, P. G. *Scaling Concepts in Polymer Physics*; Cornell University Press: Ithaca, NY, 1979.
(3) Bates, F.; Fredrickson, G. H. *Annu. Rev. Phys. Chem.* **1990**, *41*, 525.
(4) Binder, K. *Adv. Polym. Sci.* **1994**, *112*, 181.
(5) Erukhimovich, I.Ya.; Khokhlov, A. R. *Polym. Sci.* **1993**, *35*, 1522.
(6) Shakhnovich, E. I.; Gutin, A. M. *J. Phys. (Fr.)* **1989**, *50*, 1843.
(7) Leibler, L. *Macromolecules* **1980**, *13*, 1601.
(8) De Gennes, P. G. *Faraday Discuss. Chem. Soc.* **1979**, *68*, 96.
(9) Erukhimovich, I. Ya. *Polym. Sci. USSR* **1982**, *24*, 2223.
(10) Dobrynin, A. V.; Erukhimovich, I. Ya. *JETP Lett.* **1991**, *53*, 570.
(11) Fredrickson, G. H.; Milner, S. T.; Leibler, L. *Macromolecules* **1992**, *25*, 6341.
(12) Dobrynin, A. V.; Erukhimovich, I. Ya. *J. Phys. I (Fr.)* **1995**, *5*, 365.
(13) Sfatos, C. D.; Gutin, A. M.; Shakhnovich, E. I. *J. Phys. A: Math. Gen.* **1994**, *27*, L411.
(14) Swift, B. W.; Olvera de la Cruz, M. *Europhys. Lett.* **1996**, *35*, 487.
(15) Cahn, J. W.; Hilliard, J. E. *J. Chem. Phys.* **1958**, *28*, 258.
(16) Erukhimovich, I. Ya.; Dobrynin, A. V. *JETP Lett.* **1993**, *57*, 125.
(17) Dobrynin, A. V.; Erukhimovich, I. Ya. *JETP* **1993**, *77*, 307.
(18) Gutin, A. M.; Sfatos, C. D.; Shakhnovich, E. I. *J. Phys. A: Math. Gen.* **1994**, *27*, 7957.
(19) Angerman, H. J.; Ten Brinke, G.; Erukhimovich, I. *Macromolecules* **1996**, *29*, 3255.
(20) Angerman, H. J.; Ten Brinke, G.; Erukhimovich, I. *Macromol. Symp.* **1996**, *112*, 199.
(21) Dobrynin, A.V.; Erukhimovich, I. Ya. *Macromolecules* **1993**, *26*, 276.
(22) Sfatos, C. D.; Gutin, A. M.; Shakhnovich, E. I. *Phys .Rev. E* **1995**, *51*, 4727.
(23) Fredrickson, G. H.; Helfand, E. *J. Chem. Phys.* **1987**, *87*, 697.
(24) Dobrynin, A. V.; Erukhimovich, I. Ya. *J. Phys. II (Fr.)* **1991**, *1*, 1387.
(25) Panyukov, S. V.; Kuchanov, S. I. *JETP Lett.* **1991**, *54*, 501.
(26) Panyukov, S. V.; Kuchanov, S. I. *J. Phys. II (Fr)* **1992**, *2*, 1973.
(27) Erukhimovich, I. Ya.; Dobrynin, A. V. *Macromol. Symp.* **1994**, *81*, 253.
(28) Brazovskii, S. *Sov. Phys. JETP* **1975**, *41*, 85.
(29) Olvera de la Cruz, M. *Phys. Rev. Lett.* **1991**, *67*, 85.
(30) de Dominicis, C.; Martin, P. C. *J. Math. Phys.* **1964**, *5*, 1431.
(31) Nesarikar, A.; Olvera de la Cruz, M.; Crist, B. *J. Chem. Phys.*, **1993**, *98*, 7385.
(32) Dobrynin, A. V. Unpublished work, 1992.
(33) Panyukov, S. V.; Potemkin I. *JETP* **1997**, *85*, 183.
(34) Erukhimovich, I. Ya.; Angerman, H. J.; Ten Brinke, G. Unpublished work.
(35) Bouchaud, J. P.; Cates, M. E. *J. Phys. II (Fr.)* **1993**, *3*, 1171.
(36) Benoit, H.; Hadziouannou, G. *Macromolecules* **1988**, *21*, 1449.
(37) Sfatos, C. D.; Shakhnovich, E. I. *Phys. Rep.* **1997**, *288*, 77.

MA970105V